# Single Particle Protein Profiling for High Myopic Cataract Lens Capsule Tissue-derived Extracellular Vesicles Reveals Macrophage Involvement and AQP1 Correlation

Yun Su<sup>1</sup>, Xinrui Wu<sup>2</sup>, Wanzhuo He<sup>1</sup>, Chenxi Yan<sup>1</sup>, Yu<br/> Wu<sup>1</sup>, Li ${\rm Fang^1},$  Tao Guo<sup>1</sup>, and Xianqun<br/>  ${\rm Fan^1}$ 

<sup>1</sup>Shanghai Jiao Tong University School of Medicine Affiliated Ninth People's Hospital Department of Ophthalmology <sup>2</sup>Shanghai Jiao Tong University School of Medicine Affiliated Parii Herrital Department of

<sup>2</sup>Shanghai Jiao Tong University School of Medicine Affiliated Renji Hospital Department of Urology

December 10, 2024

## Abstract

High myopia stands as the primary cause of blindness globally, with cataract emerging as one of the most prevalent complications. However, the underlying mechanism of high myopic cataract remains unknown. The lens capsule is the basement membrane enclosing the lens. In this study, we hypothesized lens capsule tissue-derived EVs (Ti-EVs) play a vital role in the formation of cataract. Ti-EVs were collected from the lens capsule of high myopic and age-related cataract patients during cataract surgery, and isolated by ExoDisc. Then we performed proximity barcoding assay (PBA) for single EV analysis, which enabled us to identify the alteration of Ti-EV subpopulations associated with high myopic cataract. Our findings revealed a predominant immunity cluster within cataracts, characterized by a significantly higher abundance of macrophage-derived EVs in high myopic cataracts, which strongly correlated with the AQP1 cluster, suggesting a potential interaction between these two components in the progression of high myopic cataract. It was also observed that the eye morphogenesis cluster may also work in concert with AQP1, potentially driving the progression of high myopic cataracts through this pathway. These findings not only shed new light on the underlying mechanisms of high myopic cataract, but also pave the way for the development of novel therapeutic strategies to prevent or treat this devastating condition.

## Introduction

High myopia, characterized by a refractive error exceeding -6.00 diopters (D) or an axial length greater than 26mm, stands as a significant contributor to visual impairment globally, with its prevalence steadily rising [1]. In 2020, approximately 399 million individuals, constituting 5.1% of the world's population, were affected by high myopia. It is projected that this number could surge to nearly 938 million, accounting for 9.8% of the global population, by the year 2050 [2].

Early onset of cataract is one of the most prevalent complications associated with high myopia [3]. Many population-based studies have consistently shown a direct correlation between high myopia and an elevated risk of cataract formation, particularly with a three- to five-fold increase in the risk of nuclear cataract [4] and a 30% heightened risk of posterior subcapsular cataracts [5]. However, the exact mechanism of the precocious onset of cataract remains uncertain. One hypothesis suggests that the more pronounced vitreous liquefaction in eyes with high myopia may lead to increased exposure of the lens to oxygen from the retina, resulting in an imbalance in the oxygen defense system, and ultimately promoting cataract formation [6,7].

The lens is a transparent tissue comprising lens epithelial cells (LECs) and lens fibers cells, both enclosed

with a collagenous basement membrane known as the lens capsule. Throughout its life, LECs play pivotal roles, including differentiating into lens fibers during embryonic development, maintaining lens transparency in adulthood, and contributing to cataract formation [8]. Any disruption to the transport mechanisms, morphology, or biochemistry of the lens epithelium can alter ion concentration both inside and outside the cells, leading to fluid accumulation in the lens and ultima result in cataract formation [9]. Additionally, the lens capsule, which functions as a semipermeable membrane allowing nutrients and antioxidants to enter the lens, is also implicated in the development of lens opacification. This membrane facilitates the passive exchange of metabolic substrates and wastes between the ocular environment and lens cells [10]. However, the exact mechanism by which the lens capsule influences cataract development remains unknown.

Extracellular vesicles (EVs), which are secreted by parental cells, holds pivotal significance in facilitating intercellular communication and molecular transport [11]. These EVs are abundantly present in almost all ocular biofluids, such as aqueous humor, providing insights into the physiological and pathological conditions of their parental cells. They have also been associated with many ocular diseases, including cataract [12-14]. However, ocular biofluids contain admixtures from various sources, including serum proteins or a blend of EVs originating from different parts of the eye [15]. Furthermore, the specific proportion of EVs in the ocular biofluids that originate from particular tissues is unknown [16].

In comparison, tissue-derived EVs (Ti-EVs) are present in the extracellular interstitium and serve as wellestablished mediators of intercellular signal transduction [17]. These EVs more precisely reflect the pathophysiological characteristics and behaviors of cells, as they preserve the three-dimensional structure of tissues and cellular properties. Moreover, they are relatively uncontaminated due to their single-tissue origin, in contrast to biofluid-derived EVs [18]. While proteomics and RNA sequencing can now routinely analyze EVs and their protein and RNA contents in bulk, the inherent heterogeneity of EVs necessitates examination at the single EV level to accurately decipher the encapsulated pathophysiological information and develop promising biomarkers. Here, we utilized the proximity barcoding assay (PBA), an innovative and rapid highthroughput technique for single-EV analysis, to profile more than a hundred surface proteins on a single EV simultaneously [19]. PBA enables us to differentiate EVs based on their highly heterogeneous surface protein compositions and identify subpopulations of EVs in the human lens capsule.

In this research, PBA was performed to detect a panel of 260 proteins at single-EV resolution and subsequently classified all detected individual EVs into 7 clusters according to their proteomic features. We examined the alteration of EV clusters in high myopic cataract compared to age-related cataract as the control group. This study is poised to shed light on the complex mechanism of cataract formation. By elucidating the specific roles of EVs and their proteomic features in the development and progression of high myopic cataract, we hope to pave the way for new therapeutic strategies and interventions.

## Methods

#### Collection of lens capsule

This study received ethical approval from the Medical Science Research Ethics Committee of Shanghai Ninth People's Hospital (Approval No. SH9H-2023-T64-2). A total of sixteen patients diagnosed with cataracts were recruited from the Department of Ophthalmology, Shanghai Ninth People's Hospital. Of these, nine patients were diagnosed with age-related cataracts and served as the control group, while seven patients with high myopic cataracts comprised the experimental group. All participants, or their legal guardians, were thoroughly informed about the study and provided written informed consent. Patients' information was shown in Tables S1 in supplementary information (SI). The lens capsules were collected in the standard step of capsulorhexis during cataract surgery and preserved in a tissue storage solution for future use.

# EV isolation, purification and characterization

The lens capsules were bathed in a freshly prepared digestion solution containing 0.2% DNase I (Roche, Germany, Cat No.11284932001) and 2mg/mL collagenase D (Roche, Germany, Cat No.11088866001) with RPMI 1640 cell medium (Gibco, USA) was applied for the release of Ti-EVs. The mixture was incubated

at 37°C for 1 hour with constant agitation to ensure thorough dissociation. After digestion, the suspensions underwent a two-step centrifugation: initially at 1,000  $\times$ g for 10 minutes to remove intact cells and large particles, followed by a second centrifugation at 10,000  $\times$ g for 20 minutes to eliminate apoptotic bodies and cellular debris. The supernatants were then purified using an ExoDisc filtration device (LabSpinnerTM, Ulsan, South Korea) to isolate EVs, which were subsequently resuspended in PBS for further analysis. The size distribution and particle concentration of the purified EVs were assessed using NanoFlow CytoMetry (NanoFCM, Xiamen, China). Western blotting was performed to confirm the presence of key EV markers, including CD9, CD81 and CD63. In addition, transmission electron microscopy (TEM) imaging was used to visualize the morphology of the isolated EVs.

# Proximity barcoding assay (PBA) processing

Surface protein profiles of individual extracellular vesicles (EVs) were obtained using the PBA (ExoSeek® panel260, Secretech, Shenzhen, China), following the procedure outlined in the PBA method paper (Wu et al., 2019). In brief, EVs were first incubated with a mixture containing 260 antibodies. The antibody panel included general EV markers such as CD9, CD63, and CD81, along with biomarkers reported in the literature as potential contributors to cataract formation and mostly cellular adhesion molecules that are critical for EV targeting, cellular uptake, and signaling. Each antibody was conjugated with oligonucleotides containing unique protein tags for antibody identification, molecular tags for protein quantification, and a universal sequence for primer binding. Subsequently, the EV-antibody complexes were captured in microplate wells coated with cholera toxin subunit B (CTB), which binds to GM1 sphingolipid on the EV membrane. These complexes were then detected by individual rolling circle amplification (RCA) products, which contained DNA sequences complementary to those conjugated to the antibodies, serving as barcoding templates. All proteins from a single EV shared the same barcode. The unique protein and molecular tags, along with the RCA products (referred to as ComplexTag), were linked by annealing and PCR amplified for detection.

The libraries were sequenced on the DNBSEQ-T7 platform (MGI, Shenzhen, China) or the NovaSeq S4 system (Illumina, USA) using paired-end 150 sequencing. Raw sequencing data in bcl format were converted to FASTQ files using bcl2fastq software for downstream analysis.

#### EV proteomic data processing and analysis

Quality control of the sequencing data was performed using FastQC and the fastp package, with reads having a quality score below 20 being discarded. All data analyses were conducted in R version 4.3.1 within the RStudio environment. The EV ID–protein expression dataset was generated by counting the total number of distinct moleculeTags for each proteinTag sharing the same complexTag. Total protein abundance for each sample, referred to as the raw bulk abundance data, was determined by summing the associated moleculeTags for each protein. Differences in library size between samples were corrected using TMM normalization. For bulk data, differential expression analysis was performed using DESeq2 package and visualized through pheatmap package.

All single-EV proteomic data analysis were conducted using Seurat R package. Differential expression analysis between control and experimental groups or different clusters were performed with FindMarkers and FindAllMarkers. Functional enrichment analysis was conducted using the clusterProfiler R package (version 4.2.2), with key parameters specified as pAdjustMethod = "BH". All other parameters were left at their default settings to maintain consistency. Dimensionality reduction and clustering were performed using the FindNeighbors function (dimensions = 1:20) and FindClusters function (resolution = 0.8). The Harmony function was employed to remove batch effects during this process. The identified clusters were visualized using uniform manifold approximation and projection (UMAP). However, the high number of clusters observed suggested potential over-segmentation. To address this, we first then manually merged certain clusters based on their enriched and characteristic genes, resulting in fewer but more interpretable groups. Each group was then named according to its characteristic genes (e.g. Immunity Cluster for immune-related proteins). We used the Ro/e statistic to quantify the proportions of EVs from the experiment and control groups within individual clusters and sub-clusters, facilitating the comparison of group-specific differences in cluster

composition. In order to avoid overestimation or bias caused by highly similar proteomic profiles between different clusters by carefully controlling for statistical uncertainties through marginalization techniques, we also use BayesPrism package which could integrate results from bulk and single EV analyses. This approach enables a more comprehensive understanding of the molecular landscape by reconciling bulk-level patterns with single EV heterogeneity.

## Results

# **EV** Characterization

TEM revealed that both groups of separated EVs exhibited a cup-like structure (Figure 1B). NanoFlow CytoMetry showed that the particle sizes of EVs from both groups were distributed between 50-150 nm, with no significant difference in EVs concentration (Figure 1C-E). We quantified the tetraspanins subpopulations (CD9, CD81, CD63) in both EV samples, and the figure showed representative distribution of the CD63-positive subpopulation (Figure 1F). Both groups exhibited corresponding positive EV subpopulations. These findings confirm the successful separation of EVs.

# Single-Vesicle Landscape of Ti-EVs in Age-related and High Myopic Cataracts

Using the ExoDisc, we isolated Ti-EVs from the lens capsules of 9 patients with age-related cataracts and 7 patients with high myopic cataracts. This analysis identified a total of 260 proteins, and unsupervised clustering of their expression profiles indicated significant pathological heterogeneity between the two types of cataracts (Figure 2A). Among these proteins, 21 were differentially expressed between the groups (Figure 2B; Table S2); specifically, 13 proteins, including ABCG2, ERBB2, and CD86, were significantly enriched in high myopic cataracts, while 8 proteins were more abundant in the Ti-EVs of age-related cataracts (Figure 2C, D). Further analysis using Harmony to adjust for batch effects identified 65 subclusters comprising a total of 102,156 Ti-EVs, which were evenly distributed across both types of cataracts (Figure 2E, F; Table S3). Based on protein markers within each subcluster, we classified the Ti-EVs into seven clusters: Adhesion, AQP1, Immunity, Lysosome, Metabolize, Signal transduction, and SLC12A1&SLC12A3 (Figure 2G). Notably, each subcluster displayed distinct and clearly distinguishable protein profiles (Figure 2H).

Our data indicated that the Immunity cluster was the predominant Ti-EVs type in cataracts. Additionally, despite having two fewer samples, the Lysosome cluster was more prevalent in pathological cataracts (Figure 2I). There were no significant differences in Ti-EV between samples, and each cluster was well represented across samples, suggesting that the observed patterns are consistent and not significantly affected by individual sample variability (Figure 2J). The Ro/e values for the Lysosome, AQP1, Immunity, and SLC12A1&SLC12A3 clusters were higher in high myopic cataract samples, indicating these ones may potential pathogenic factors (Figure 2K). Notably enriched proteins in the Lysosome cluster included CDH17, LAMP1, HLA-DRA, and IL6 (Figure S1A), while AQP1 and CDCP1 were enriched in the AQP1 cluster (Figure S1B), with a high correlation observed between these two groups (Figure S1C). Interestingly, AB-CG2, ERBB2, and CD86 were primarily located in the Immunity cluster, suggesting a possible role in the progression of high myopic cataracts.

## Distribution and Function of Immunity Cluster from all Ti-EVs in Cataracts

We subset 42,199 Ti-EVs from Immunity cluster, including Macrophage, T, HAVCR1, and other clusters (Figure 3A). The Macrophage-derived cluster exhibited high expression of CD68, MRC1, CD80, CD86, and CD14, while the T cell-derived cluster was marked by high expression of CD3D and CD3E (Figure 3B). Functionally, the T cell-derived cluster was primarily involved in pathways related to cell adhesion mediated by integrins and the positive regulation of fibroblast migration, whereas the increased presence of Macrophage-derived cluster appeared to respond to bacterial invasion (Figure 3C). It is noting that the other immune-related Ti-EV cluster comprised the majority of the cataract immunity landscape (Figure 3D, E), and further division was deemed unnecessary as their protein contents showed no significant differences.

Notably, the Ro/e value for Macrophage-derived Ti-EVs cluster was higher in high myopic cataracts, while

the value for T cell-derived Ti-EVs cluster was higher in age-related cataracts (Figure 3F). Additionally, the total expression of the 264 proteins in each Ti-EV correlated highly with overall protein expression (R=0.908; Figure 3G). Using BayesPrism to deconvolute individual Ti-EV and project this information onto total proteins, we observed that the Macrophage-derived cluster was more abundant in high myopic cataracts and showed a strong correlation with the AQP1 cluster (R=0.680, P=0.004; Figure 3I, J). Interestingly, among proteins linked to cataract progression, AQP1, ITGAV, and ITGB1 were significantly upregulated in Ti-EVs, with AQP1 more prominent in high myopic cataracts (Figure S1D). These findings suggest that Macrophage-derived Ti-EVs and AQP1 in Ti-EVs may synergistically contribute to drive the progression of high myopic cataracts.

# Role of Macrophage-Derived Ti-EVs in the Progression of High Myopic Cataracts

A total of 6,161 Ti-EVs were classified as Macrophage-derived based on their protein expression profiles. Initially divided into 11 subclusters (Table S4), these were later consolidated into 9 Macrophage subclusters with distinct functions: Healing, Eye morphogenesis, Cell recognition, DC APC, Cell killing, T cell differentiation, Immunoglobulin, Protein localization, and Adhesion (Figure 4A; Table S5). In terms of prevalence, Macrophage-derived Ti-EVs were more common in senile cataracts, largely due to differences in sample size (Figure 4C). Additionally, the subclusters were evenly distributed across all samples, suggesting low sample heterogeneity (Figure 4D). Notably, the Eye morphogenesis, Cell killing, Adhesion, and T cell differentiation subclusters exhibited higher Ro/e values in pathological cataracts (Figure 4E), indicating that these subclusters may play a role in contributing the development of high myopic cataracts.

## Synergistic Role of Macrophage-Derived Ti-EVs and AQP1 in Promoting Eye Morphogenesis

Our findings indicated that the Eye morphogenesis cluster was characterized by high expression of HAVCR1, CPM, and MRC1; the Cell killing cluster by CDH15, PCDH1, MICA, and APOE; the Adhesion cluster by PCDH8, CDH3, CLDN10, VCAM1, and CDH11; and the T cell differentiation cluster by CD28 and CD80 (Figure 5A). Deconvolution analysis revealed a significant association among the Eye morphogenesis, Cell killing, and AQP1 subclusters (Figure 5B; Table S6). Additionally, Eye morphogenesis and Cell killing subclusters were more frequently observed in high myopic cataracts, suggesting a potential cooperative mechanism (Figure 5C). To further investigate the interactions between the AQP1 and Macrophage clusters, we analyzed AQP1 expression within macrophage subclusters and found it to be significantly elevated in the Eye morphogenesis cluster, suggesting that the Eye morphogenesis cluster may work in concert with AQP1, potentially driving the progression of high myopic cataracts through this pathway.

# Discussion

The results of this study demonstrate that the immunity cluster predominates in cataracts, with a higher abundance of macrophage-derived Ti-EVs in high myopic cataracts, which strongly correlates with the AQP1 cluster. It was also observed that the eye morphogenesis cluster may also work in concert with AQP1, potentially driving the progression of high myopic cataracts through this pathway.

These findings were for the first time elucidate the mechanism of cataract formation from the perspective of Ti-EVs derived from the lens capsule. Ti-EVs constitute a specific class of extracellular vesicles that originate from and reside within the interstitial spaces of tissues. These vesicles are secreted by various cell types within tissues and play pivotal roles in intercellular communication and the regulation of tissue micro-environments. Notably, Ti-EVs derived from lens capsules exhibit remarkable tissue specificity, maintaining their identity despite the complex ocular environment. This specificity enables them to accurately reflect the pathophysiological characteristics and behaviors of the cells within their original tissues. Consequently, this tissue-specific nature of these Ti-EVs allows for a precise analysis of their components, which will facilitate a deeper understanding of the pathological processes underlying high myopic cataract.

In the realm of cataract research, such as high myopic cataract, the lens capsules hold a paramount significance, serving as a cornerstone in unraveling the complexities of the disease. However, the quantity of EVs that can be obtained from these tissues is minuscule due to their delicate thinness and minute size, making the efficient extraction and in-depth analysis of their contents an essential endeavor. To address this challenge, our research team innovatively adopted a cutting-edge methodology that integrates microfluidic technology with PBA. This combination allowed us to meticulously extract and meticulously analyze Ti-EVs. Leveraging the precision and sensitivity of these advanced techniques, we were able to achieve a remarkable breakthrough: successfully isolating a median of 6.24\*10^7 particles/mL EVs from a mere single capsular membrane. Furthermore, utilizing the powerful PBA platform, we were able to detect and identify a comprehensive list of 264 proteins, providing us with invaluable insights into the composition and function of these EVs.

In our findings, the immunity cluster holds a dominant position in the development of cataracts. The interplay between immune response and cataract formation has been increasingly acknowledged. Immune responses involving cytokines and inflammatory mediators have been implicated in the process of cataract formation [20]. Recent research has underscored the significance of the immune disfunction caused by systemic inflammation, notably from conditions such as periodontitis, in intensifying cataract development [20-22]. In a large-scale national survey involving 11,205 participants, Huang et al. investigated the systemic immune-inflammation index (SII), which was determined by neutrophils, lymphocytes, and platelets. They observed that a high SII level exceeding 500\*10<sup>9</sup>/L was positively associated with cataract development among women, contributing valuable insights into the relationship between high SII levels and risk of cataract in adults in the United States [20]. Yeh et al. revealed that periodontitis can provoke systemic inflammation and oxidative stress, both of which are linked to the onset of various eye diseases, including cataracts [21]. This implies that immune disruptions triggered by oral microbiome from periodontitis may play a role in the oro-optic-network and promote the development of cataract.

In this study, it was observed that the lens capsule of patients with high myopic cataract contained a significantly higher abundance of macrophage-derived Ti-EVs. This finding is consistent with earlier research, which suggested that macrophage activation, recruitment, and the subsequent macrophage-mediated inflammation play pivotal roles in the development of lens opacification [23-25]. Previous studies have demonstrated that, in the aqueous humor of myopic eyes, there is an elevated presence of proinflammatory cytokines [24], such as interleukin-6 (IL-6) and matrix metalloproteinases (MMPs), which could create an environment that favors macrophage activation and recruitment. Similarly, the increased level of oxidative stress due to higher oxygen tension around the lens could also activate macrophages and other immune cells [25], leading to an influx of macrophages into the lens capsule. The activated macrophages, in turn, release EVs, which interacted with lens epithelial cells, inducing changes in their behavior, and contributing to the opacity of the lens. The precise mechanisms by which Ti-EVs mediate lens opacification are still being elucidated, but it is clear that the presence of these vesicles in the lens capsule is closely associated with the development of high myopic cataract.

Aquaporin 1 (AQP1) is a membrane-embedded water channel protein that play a crucial role in facilitating the passive transport of water molecules across cellular membranes along osmotic gradients. Studies have shown that AQP1 is involved in the maintenance of osmotic balance and the regulation of cellular hydration, making it an essential component for proper cellular function [26-28]. In the lens, AQP1 also performs a vital function by enabling the efficient movement of water. This facilitates the precise control of water content within lens fibers, which is critical for maintaining the lens' transparency and refractive properties. The delicate balance of water movement regulated by AQP1 ensures that the lens remains clear and functions optimally, allowing for clear vision [29]. When the normal function of AQP1 is compromised, it can lead to alterations in the hydration state of lens fibers, resulting in the opacity of the lens [30]. An increased level of AQP1 protein expression was noted in the lens epithelial cells of cataract patients [31].

AQP1 is also known to play a crucial role in the regulation of macrophage function, particularly in modulating inflammatory responses. Studies have shown that AQP1 can attenuate macrophage-mediated inflammation by inhibiting the activation of p38 mitogen-activated protein kinase (MAPK) pathways, which are critical in the inflammatory response [32]. This suggests that AQP1 may help maintain a balance in macrophage polarization, potentially preventing excessive inflammation that could exacerbate conditions like high myopia

and its associated cataracts [33]. In addition, the polarization of macrophages towards an M2 phenotype, which is associated with tissue repair and anti-inflammatory responses, can also be influenced by AQP1 levels [34], which would be beneficial for initial repair but may also lead to excessive inflammation and fibrosis if not properly regulated, contributing to cataract formation. We further analyzed AQP1 expression within macrophage subclusters and discovered a notable increase in the Eye morphogenesis cluster, which was characterized by high expression of HAVCR1, CPM, and MRC1, indicating potential collaboration between this cluster and AQP1.

Based on our findings, we postulate that the development of high myopic cataract could be attributed to a complex interplay of multiple factors, such as change in the ocular morphology, that disrupt the normal functioning of macrophages during the progression of high myopia. As a result, the altered macrophage function could lead to dysregulation in the expression of AQP1, which disrupt the lens homeostasis, promoting the onset and progression of cataract. Therefore, our hypothesis suggests a potential causal link between macrophage dysfunction, altered AQP1 expression, and the development of high myopic cataract, highlighting the need for further research to elucidate the underlying mechanisms and explore potential therapeutic interventions.

A key limitation of this study is the small sample size, which may restrict the generalizability of our findings. A larger sample size would be necessary to confirm the statistical significance and robustness of our results, allowing for more accurate and reliable conclusions to be drawn. In addition, the number of proteins that can be detected by PBA are limited, which prevented us from identifying all relevant proteins involved in the processes we investigated. Future research could explore the utilization of more advanced techniques or platforms, could provide a more comprehensive understanding of the biological mechanisms at play. Moreover, the potential mechanisms proposed in our study require further biological validation to confirm their validity. The markers identified need to undergo clinical validation to assess their therapeutic potential in real-world settings. This validation process is crucial for translating our research findings into practical applications that can benefit patients and improve clinical outcomes.

In summary, this study investigated the alteration in subpopulation patterns of single Ti-EVs derived from the lens capsules of patients with high myopic cataract and age-related cataract by PBA. By analyzing their protein profiling, we observed a significantly higher abundance of macrophage-derived Ti-EVs in high myopic cataracts, which strongly correlates with the AQP1 cluster. The interaction between macrophage and AQP1 may provide new insights into the underlying mechanisms driving the progression of high myopic cataracts.

#### Funding

This work was supported by the National Natural Science Foundation of China (82371102, 82371054), Shanghai Key Clinical Specialty, Shanghai Eye Disease Research Center (2022ZZ01003), Science and Technology Commission of Shanghai (20DZ2270800, 23JC1402402), Shanghai Pujiang Program (22PJD036), and Shanghai Jiao Tong University 2030 Initiative (WH510363002/005).

## Notes

The authors declare no competing financial interest.

# Figure Legend

Figure 1 Collection of Lens Capsules, Incubation, Isolation and Characterization of Ti-EVs from Lens Capsules. A. Schematic illustration of collection of lens capsules during cataract surgery and the following incubation and isolation of Ti-EVs from the lens capsules. B. The structure of the separated EVs was examined using TEM. Scale bar represented 200 nm in figures. C. The size distribution of separated EVs demonstrated by nFCM. D. The concentration of separated EVs. E. The characters of the separated EVs were examined using nFCM with specific antibodies against EV membrane-specific proteins CD63. Unpaired t-test. F. Proportion of EV membrane-specific proteins in both groups, including CD9, CD81, CD63.

Figure 2 Immune Cell Derived EVs in the Progression of High Myopic Cataract. A. Heatmap

displaying differential proteins in EVs derived from the lens tissues of age-related and high myopic cataract. B. Dot plot showing the ranking of differential proteins in EVs from the lens tissues. C. Bar plot illustrating the expression levels (TMM Normalized) of ABCG2, ERBB2, and CD86 in EVs. D. Heatmap presenting the expression levels of statistically significant differential proteins in EVs. E. Overview of EVs derived from the lens tissues of age-related and high myopic cataract. F. Overview of the origins of EVs derived from the lens tissues, as determined by PBA. G. Panorama of annotated EVs subclusters derived from the lens tissues. H. Heatmap showing the expression of marker proteins in each subcluster. I. Proportional chart depicting the contribution of EVs from different cell sources in age-related and high myopic cataract. J. Proportional chart showing the contribution of EVs from different cell sources across individual samples. K. Distribution of Ro/e values for EV subclusters in age-related and high myopic cataract. L. Expression levels of ABCG2, ERBB2, and CD86 across different EVs.

Figure 3 Macrophage-Derived EVs Synergistically Promote the Development of High Myopic Cataracts via AQP1. A. UMAP plot illustrating the global distribution of immune cell derived EVs. B. Dot plot showing marker proteins for different immune cell-derived EV subclusters. C. Heatmap displaying the highly expressed proteins and their associated pathways in immune cell derived EV subclusters. D. Proportional chart representing the distribution of immune cell derived EVs in age-related and high myopic cataract. E. Proportional chart showing the contribution of immune cell derived EVs in individual samples F. Distribution of Ro/e values for immune cell derived EV subclusters in age-related and high myopic cataract. G. Dot plot comparing shared protein expression between single EVs and bulk proteomics. H. Distribution of immune EV subclusters in age-related and high myopic cataract using deconvolution. J. Dot plot showing the correlation between AQP1 expression and immune cell derived EVs.

Figure 4 Macrophage-Derived EVs Facilitate High Myopic Cataract Development through Eye Morphogenesis. A. UMAP plot illustrating the distribution of macrophage-derived EV subclusters. B. Heatmap showing the highly expressed proteins and associated pathways in macrophage-derived EV subclusters. C. Proportional chart showing the distribution of macrophage-derived EVs in age-related and high myopic cataract. D. Proportional chart illustrating the contribution of macrophage-derived EVs across individual samples. E. Distribution of Ro/e values for macrophage-derived EV subclusters in age-related and high myopic cataract.

Figure 5 AQP1 in Macrophage-Derived EVs Synergistically Promotes High Myopic Cataract Progression via Eye Morphogenesis . A. Volcano plot illustrating differential proteins in macrophagederived EV subclusters in age-related and high myopic cataract. B. Correlation pie chart for macrophagederived EV subclusters. C. Distribution of different functional subclusters of macrophage-derived EVs in age-related and high myopic cataract. D. Violin plot showing the expression levels of AQP1 in different functional subclusters of macrophage-derived EVs.

# References

Flitcroft DI, He M, Jonas JB, Jong M, Naidoo K, Ohno-Matsui K, Rahi J, Resnikoff S, Vitale S, Yannuzzi L. IMI - Defining and Classifying Myopia: A Proposed Set of Standards for Clinical and Epidemiologic Studies. Invest Ophthalmol Vis Sci. 2019 Feb 28;60(3):M20-M30.

[2] Holden BA, Fricke TR, Wilson DA, Jong M, Naidoo KS, Sankaridurg P, Wong TY, Naduvilath TJ, Resnikoff S. Global Prevalence of Myopia and High Myopia and Temporal Trends from 2000 through 2050. Ophthalmology. 2016 May;123(5):1036-42.

[3] Du Y, Meng J, He W, Qi J, Lu Y, Zhu X. Complications of high myopia: An update from clinical manifestations to underlying mechanisms. Adv Ophthalmol Pract Res. 2024 Jun 21;4(3):156-163.

[4] Kanthan GL, Mitchell P, Rochtchina E, et al. Myopia and the long-term incidence of cataract and cataract surgery: the Blue Mountains Eye Study. Clin Exp Ophthalmol 2014; 42:347 – 353.

[5] Pan CW, Boey PY, Cheng CY, et al. Myopia, axial length, and age-related cataract: the Singapore Malay eye study. Invest Ophthalmol Vis Sci 2013; 54:4498 – 4502.

[6] Holekamp NM. The vitreous gel: more than meets the eye. Am J Ophthalmol. 2010 Jan;149(1):32-6.

[7] Harocopos GJ, Shui YB, McKinnon M, Holekamp NM, Gordon MO, Beebe DC. Importance of vitreous liquefaction in age-related cataract. Invest Ophthalmol Vis Sci. 2004 Jan;45(1):77-85.

[8] Liu Z, Huang S, Zheng Y, Zhou T, Hu L, Xiong L, Li DW, Liu Y. The lens epithelium as a major determinant in the development, maintenance, and regeneration of the crystalline lens. Prog Retin Eye Res. 2023 Jan;92:101112.

[9] Spector A, Wang GM, Wang RR, Garner WH, Moll H. The prevention of cataract caused by oxidative stress in cultured rat lenses. I. H2O2 and photochemically induced cataract. Curr Eye Res. 1993 Feb;12(2):163-79.

[10] Huang D, Xu C, Guo R, Ji J, Liu W. Anterior lens capsule: biomechanical properties and biomedical engineering perspectives. Acta Ophthalmol. 2021 May;99(3):e302-e309.

[11] Yanez-Mo M, Siljander PR, Andreu Z, Zavec AB, Borras FE, Buzas EI, Buzas K, Casal E, Cappello F, Carvalho J, Colas E, Cordeiro-da Silva A, Fais S, Falcon-Perez JM, Ghobrial IM, Giebel B, Gimona M, Graner M, Gursel I, Gursel M, Heegaard NH, Hendrix A, Kierulf P, Kokubun K, Kosanovic M, Kralj-Iglic V, Kramer-Albers EM, Laitinen S, Lasser C, Lener T, Ligeti E, Linē A, Lipps G, Llorente A, Lötvall J, Manček-Keber M, Marcilla A, Mittelbrunn M, Nazarenko I, Nolte-'t Hoen EN, Nyman TA, O'Driscoll L, Olivan M, Oliveira C, Pállinger É, Del Portillo HA, Reventós J, Rigau M, Rohde E, Sammar M, Sánchez-Madrid F, Santarém N, Schallmoser K, Ostenfeld MS, Stoorvogel W, Stukelj R, Van der Grein SG, Vasconcelos MH, Wauben MH, De Wever O. Biological properties of extracellular vesicles and their physiological functions. J Extracell Vesicles. 2015 May 14;4:27066.

[12] Gao C, Liu X, Fan F, Yang JN, Zhou XY, Mei HJ, Lin XL, Luo Y. Exosomal miR-29b found in aqueous humour mediates calcium signaling in diabetic patients with cataract. Int J Ophthalmol. 2021 Oct 18;14(10):1484-1491.

[13] Guo C, Zhang J, Wang J, Su L, Ning X, Guo Y, Han J, Ma N. Vascular endothelial cell-derived exosomal miR-1246 facilitates posterior capsule opacification development by targeting GSK-3β in diabetes mellitus. Exp Eye Res. 2023 Jun;231:109463.

[14] Wang R, Li J, Zhang X, Zhang X, Zhang X, Zhu Y, Chen C, Liu Z, Wu X, Wang D, Dongye M, Wang J, Lin H. Extracellular vesicles promote epithelial-to-mesenchymal transition of lens epithelial cells under oxidative stress. Exp Cell Res. 2021 Jan 1;398(1):112362.

[15] Su Y, Chen M, Xu W, Gu P, Fan X. Advances in Extracellular-Vesicles-Based Diagnostic and Therapeutic Approaches for Ocular Diseases. ACS Nano. 2024 Aug 27;18(34):22793-22828.

[16] Crescitelli R, Lässer C, Lötvall J. Isolation and characterization of extracellular vesicle subpopulations from tissues. Nat Protoc. 2021 Mar;16(3):1548-1580.

[17] Lee JC, Ray RM, Scott TA. Prospects and challenges of tissue-derived extracellular vesicles. Mol Ther. 2024 Sep 4;32(9):2950-2978.

[18] Li SR, Man QW, Gao X, Lin H, Wang J, Su FC, Wang HQ, Bu LL, Liu B, Chen G. Tissue-derived extracellular vesicles in cancers and non-cancer diseases: Present and future. J Extracell Vesicles. 2021 Dec;10(14):e12175.

[19] Wu D, Yan J, Shen X, Sun Y, Thulin M, Cai Y, Wik L, Shen Q, Oelrich J, Qian X, Dubois KL, Ronquist KG, Nilsson M, Landegren U, Kamali-Moghaddam M. Profiling surface proteins on individual exosomes using a proximity barcoding assay. Nat Commun. 2019 Aug 26;10(1):3854. doi: 10.1038/s41467-019-11486-1. PMID: 31451692; PMCID: PMC6710248.

[20] Huang J, Wu H, Yu F, Wu F, Hang C, Zhang X, Hao Y, Fu H, Xu H, Li R, Chen D. Association between systemic immune-inflammation index and cataract among outpatient US adults. Front Med (Lausanne). 2024 Sep 18;11:1469200.

[21] Yeh LJ, Shen TC, Sun KT, Lin CL, Hsia NY. Periodontitis and Subsequent Risk of Cataract: Results from Real-World Practice. Front Med (Lausanne). 2022 Feb 4;9:721119.

[22] Wen R, Xi YJ, Zhang R, Hou SJ, Shi JY, Chen JY, Zhang HY, Qiao J, Feng YQ, Zhang SX. Prescription glucocorticoid medication and iridocyclitis are associated with an increased risk of senile cataract occurrence: a Mendelian randomization study. Aging (Albany NY). 2024 Jun 26;16(12):10563-10578.

[23] Yuan J, Wu S, Wang Y, Pan S, Wang P, Cheng L. Inflammatory cytokines in highly myopic eyes. Sci Rep. 2019 Mar 5;9(1):3517.

[24] Zhu X, Zhang K, He W, Yang J, Sun X, Jiang C, Dai J, Lu Y. Proinflammatory status in the aqueous humor of high myopic cataract eyes. Exp Eye Res. 2016 Jan;142:13-8.

[25] Zhu X, Li D, Du Y, He W, Lu Y. DNA hypermethylation-mediated downregulation of antioxidant genes contributes to the early onset of cataracts in highly myopic eyes. Redox Biol. 2018 Oct;19:179-189.

[26] Devuyst O. Aquaporin-1 and Osmosis: From Physiology to Precision in Peritoneal Dialysis. J Am Soc Nephrol. 2024 Nov 1;35(11):1589-1599.

[27] Zhou Z, Zhan J, Cai Q, Xu F, Chai R, Lam K, Luan Z, Zhou G, Tsang S, Kipp M, Han W, Zhang R, Yu ACH. The Water Transport System in Astrocytes-Aquaporins. Cells. 2022 Aug 18;11(16):2564.

[28] Schey KL, Petrova RS, Gletten RB, Donaldson PJ. The Role of Aquaporins in Ocular Lens Homeostasis. Int J Mol Sci. 2017 Dec 12;18(12):2693.

[29] Zhao M, Zhao S, Tang M, Sun T, Zheng Z, Ma M. Aqueous Humor Biomarkers of Retinal Glial Cell Activation in Patients With or Without Age-Related Cataracts and With Different Stages of Diabetic Retinopathy. Invest Ophthalmol Vis Sci. 2022 Mar 2;63(3):8.

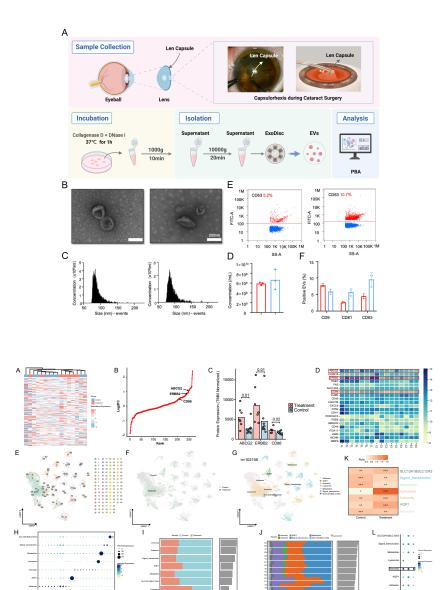
[30] Xia CH, Lin W, Li R, Xing X, Shang GJ, Zhang H, Gong X. Altered Cell Clusters and Upregulated Aqp1 in Connexin 50 Knockout Lens Epithelium. Invest Ophthalmol Vis Sci. 2024 Sep 3;65(11):27.

[31] Barandika O, Ezquerra-Inchausti M, Anasagasti A, Vallejo-Illarramendi A, Llarena I, Bascaran L, Alberdi T, De Benedetti G, Mendicute J, Ruiz-Ederra J. Increased aquaporin 1 and 5 membrane expression in the lens epithelium of cataract patients. Biochim Biophys Acta. 2016 Oct;1862(10):2015-21.

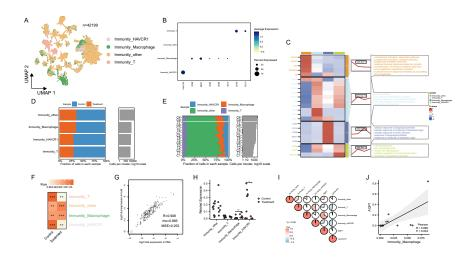
[32] Li B, Liu C, Tang K, Dong X, Xue L, Su G, Zhang W, Jin Y. Aquaporin-1 attenuates macrophage-mediated inflammatory responses by inhibiting p38 mitogen-activated protein kinase activation in lipopolysaccharide-induced acute kidney injury. Inflamm Res. 2019 Dec;68(12):1035-1047.

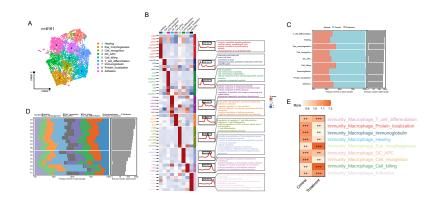
[33] Tyteca D, Nishino T, Debaix H, Van Der Smissen P, N'Kuli F, Hoffmann D, Cnops Y, Rabolli V, van Loo G, Beyaert R, Huaux F, Devuyst O, Courtoy PJ. Regulation of macrophage motility by the water channel aquaporin-1: crucial role of M0/M2 phenotype switch. PLoS One. 2015 Feb 26;10(2):e0117398.

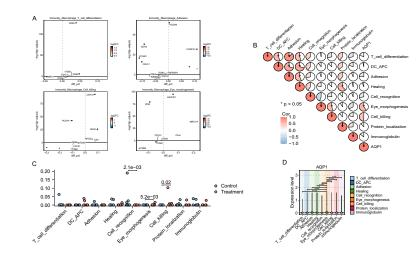
[34] Liu C, Li B, Tang K, Dong X, Xue L, Su G, Jin Y. Aquaporin 1 alleviates acute kidney injury via PI3K-mediated macrophage M2 polarization. Inflamm Res. 2020 May;69(5):509-521.



... 100000 100000 100000 10000 10000 10000 10000 10000 100000







'doi.org/10.22541/au.173379815.53340841/v1 — This is a preprint

